RSC Advances

ROYAL SOCIETY OF CHEMISTRY

www.rsc.org/advances

Effects of Fluorine Ions on the Formation and Photocatalytic Activities of SnO_2 Nanoparticles with Small Sizes

Tingting Hao, Guoe Cheng*, Hanzhong Ke, Yujie Zhu, Yangming Fu

Faculty of Material & Chemistry, China University of Geosciences, Wuhan, Hubei 430074, PR China

Abstract: SnO_2 nanoparticles with small sizes were synthesized by a simple hydrothermal route with existence of different dosages of fluorine ions. These nanoparticles all showed typical rutile phase and excessive dosage of fluorine ions would result in other crystallographic phase. The average diameters of as-prepared products were all smaller than 4 nm. The introduction of fluorine ions showed little influence on the morphologies and crystallite sizes, but enhanced the crystallization of rutile phase and promoted the growth of SnO_2 crystallites. XPS patterns showed that some introduced fluorine ions were physically adsorbed on the surface of SnO_2 crystals, but not doped in the lattice. The photocatalytic activities were tested with photodecomposition of Rhodamine B (RhB) under a 300 W high-pressure mercury lamp. The results indicated that proper amount of fluorine ions on the surface of SnO_2 nanoparticles caused significant enhancement of their photocatalytic activities.

Keywords: SnO_2 nanoparticles Fluorine ions Photocatalytic activity Small diameters

1. Introduction

In recent years, semiconductor photocatalytic materials have drawn wide attention from researchers due to their wide potential applications in water, air purification and solar energy conversion and so on.

* To whom correspondence should be addressed. E-mail address: chengguoe68@aliyun.com. Phone: 86-27-67883731. Fax: 86-27-67883731

SnO_2, as a stable n-type wide band gap semiconductor (Eg = 3.6 eV), is well-known for potential applications in transparent electrodes, gas sensors, storage applications and solar cells [1-5]. Recently, photocatalytic activities of SnO_2 nanocrystals have been reported by a few papers [6-11]. Li *et al.* report that V-shaped SnO_2 bipods show unprecedented visible-light-driven photocatalytic activities [7]. Meanwhile SnO_2 nanostructures with various morphologies and microstructures exhibit diverse photocatalytic activities [8-11]. These results reveal that SnO_2 nanocrystals have a great potential prospect on photocatalytic activities. However, comparing with TiO_2 nanostructures, photocatalytic performances of SnO_2 nanocrystals still have much room for improvement [12-17]. Enhancing the photocatalytic activities of SnO_2 nanostructures is still a major challenge and worth to further study.

In general, doping or introduced in the additive can improve the microstructure of SnO_2 nanomaterials, and affect the macroscopic performances, such as electricity, optics, magnetism and gas sensitive performances, especially the photocatalytic activities. With doping or introduced in the additive, it makes a reduction of the recombination rate of photogenerated electrons and holes, resulting in the enhancement of photoactivity [18-19]. SnO_2/ZnO composite has been reported to exhibit a significant enhancement of photocatalytic capability toward degrading RhB compared to undoped m-SnO_2 [20]. Metal elements doping of SnO_2 photocatalysts have been reported frequently, such as In, Sb, Au, Fe, Cd, Ni, Pd etc. [21-27]. However, few papers are about nonmetal elements doping or introducing fluorine ion into SnO_2 nanostructures. In fact, studies have shown that doping or introducing fluorine ion can promote the growth of active crystal plans, reduce the recombination rate of photogenerated electrons and holes, and improve photocatalytic performances of TiO_2 nanocrystals [28-34]. Park *et al.* report that F-TiO_2 is more effective than pure TiO_2 for the photocatalytic oxidation of Acid Orange 7, which presents the degradation

of Acid Orange 7 reaches 100% degradation rate within 40 min under UV irradiation [35]. In this work, we report the simply hydrothermal synthesis of SnO_2 nanoparticles with small diameters in water with assistance by sodium fluoride. Different dosages of fluorine ions are employed to study the effects of fluorine ions on the formation and photocatalytic activities.

2. Experimental section

2.1. Preparation

All the chemicals used in this experiment were analytical grade and were used without further purification. In a typical synthesis, 1.05 g of tin (IV) chloride pentahydrate ($SnCl_4 \cdot 5H_2O$) was dissolved in 56 mL of distilled water under stirring at room temperature and the transparent clear solution was obtained. Then the above solution was transferred into a 70 mL stainless steel Teflon-lined autoclave. After maintaining in an oven at 180 °C for 5 h, the autoclave was cooled down to room temperature naturally. White precipitate was collected and washed with distilled water and absolute ethanol by centrifugation for several times successively, followed by drying in air at 80 °C for 24 h. The as-obtained product was called **Sn-0F**. On this basis, different dosages of sodium fluoride (NaF) were dissolved together with $SnCl_4 \cdot 5H_2O$ into distilled water to investigate the effect of the fluorine ion on SnO_2 nanostructures. The molar ratios of NaF to $SnCl_4 \cdot 5H_2O$ (R_F) were adjusted to 0.5:1, 1:1, 2:1, 3:1 and 4:1, and the as-obtained products were named as **Sn-1/2F**, **Sn-F**, **Sn-2F**, **Sn-3F** and **Sn-4F**, respectively.

2.2. Characterizations

The crystalline phase of the SnO_2 powders were carried out by an X-ray diffractometer (XRD, Bruker Axs D8-Focus, Cu kα radiation with λ = 1.5406 Å). Surface chemical analysis of the samples was

conducted on an X-ray photoelectron spectroscope (XPS, Multilab 2000). All binding energies were referenced to the C 1s peak with a binding energy of 284.7 eV of the surface adventitious carbon. The microscopic nanostructures were measured using a FEI Tecnai G^2 20 transmission electron microscopy (TEM) at an acceleration voltage of 200 kV.

2.3. Photoactivity Measurement

The photocatalytic activities were tested by photochemical reactions instrument (BL-GHX-IV) and UV–vis adsorption spectra (UV-1801). RhB was used as a probe molecule to research the photocatalytic activities of SnO_2 nanorods. The experiments were carried out as follows: 50 mg of the samples were dispersed in 50 mL of 10 $mg \cdot L^{-1}$ RhB solution in a quartz tube. Prior to illumination, the suspensions were magnetically stirred in the dark for 1 h to establish adsorption–desorption equilibrium. Subsequently, the suspension was irradiated under a 300 W high-pressure mercury lamp. Every time 5 mL of the above solution was taken out and centrifuged before UV-vis analysis. UV–vis adsorption spectra were recorded at certain time intervals (10 min) to monitor the process.

3. Results and Discussion

The XRD patterns of the as-obtained products are all shown in Fig. 1. All the diffraction peaks of the sample **Sn-0F** can be indexed to the rutile phase SnO_2 (cassiterite, JCPDS card No. 41-1445, space group: $P4_2/mnm$) with tetragonal lattice constant a=4.738 Å and c=3.187 Å. When different dosages of NaF were introduced, the obtained samples also show tetragonal SnO_2 with rutile structure. However, the widths of the diffraction peaks can be found to become narrower steadily with the dosages of fluorine ion increased, indicating that the introducing of fluorine ion can improve crystallinity of SnO_2 nanoparticles. In fact, we have found that the introduction of fluorine ion can also increase yield of SnO_2 nanoparticles. The yield of

those samples contained fluoride ion is at least twice as much as that of the samples without fluoride ion. However, with R_F increased to 4:1, some impure peaks are found to exist in SnO_2 nanocrystals (marked with *). Maybe the fluorine ions are incorporated into the SnO_2 lattice which results in the formation of new crystallographic phase. Yu *et al.* also found that fluorine ions doping in TiO_2 nanocrystallines enhanced the crystallization of anatase phase and promoted the growth of crystallites, even can changed the crystalline phase [29].

TEM images illustrate microscopic nanostructures of the as-obtained products (Fig. 2). As can be seen from Fig. 2, the samples are all composed of uniform SnO_2 nanoparticles with small sizes. The average diameters of all samples are smaller than 4 nm. The introduction of fluorine ions shows little influence on the morphology and crystallite sizes. The high resolution transmission electron microscopy (HRTEM) of the products **Sn-0F** and **Sn-2F** are presented in Fig. 3. As can be seen from the Fig. 3, the lattice fringes in the HRTEM image further confirm the single-crystal nature of the SnO_2 nanoparticles. The crystal spacing between adjacent lattice planes is 0.334 nm, corresponding to (110) planes of rutile SnO_2.

XPS is also carried out to investigate the surface compositions and chemical state. Their corresponding binding energy values are used for quantitative measurements of the elements present in the material [36]. The results of the samples **Sn-0F** and **Sn-2F** are shown in Fig. 4, respectively. The XPS patterns show that the **Sn-0F** contains only Sn and O without any trace impurities except C elements (Fig. 4a). The peaks of the **Sn-0F** observed at 486.3 eV and 495.2 eV (Fig. 4b) are attributable to Sn $3d_{5/2}$ and Sn $3d_{3/2}$, 530.6 eV to O 1s, respectively (Fig. 4c). The C element could be attributed to the adventitious carbon-based contaminant. The binding energy of Sn $3d_{5/2}$ is 486.3 eV for the **Sn-0F** (Fig. 4b), slightly lower than that of tin oxide (>486.4 eV). According to Peng *et al.*, this result suggests that these

nanoparticles are oxygen deficient because the oxygen deficiency can decrease the binding energy of Sn [37]. The peak with an O 1s binding energy around 530.6 eV corresponds to the Sn-O-Sn bonds, indicating that the oxygen atoms exist as O^{2-} species in the compounds (Fig. 4c) [38]. Quantification gives an atomic ratio of Sn and O of 1:1.518 which also confirms the existence of oxygen vacancies. In comparision, besides Sn, O, and C elements, the **Sn-2F** contains F elements as well (Fig. 4a). The Fig. 4d shows the binding energy of F 1s is 684.5 eV which is attributed to the fluorine ions physically adsorbed on the surface of SnO_2. The surface fluoride could be formed by ligand exchange reaction between fluorine ions and the surface hydroxyl group on the surface of crystals [39]. No other peak can be found to be attributed to the incorporated fluorine ions in SnO_2 lattice.

The UV-Vis DRS of all samples are presented in Fig.5 to detect their optical absorption properties and the information on their band gap. All the composite photocatalysts have a strong absorption feature in the UV region (below 400 nm) and the visible light absorption is not observed. In comparison with the sample **Sn-0F**, the absorption edges of the samples **Sn-F**, **Sn-2F**, **Sn-3F** and **Sn-4F** are blue-shifted while the absorption edge of **Sn-1/2F** shows a slight red-shift. With the increase of fluoride ion, the blue-shift phenomenons were more greatly increased. Moreover, we can observe that the samples **Sn-0F**, **Sn-1/2F, Sn-F** and **Sn-2F** have a broader absorption feature while the samples **Sn-3F** and **Sn-4F** can only absorb the UV light below 375 nm.

To understand the effect of particle size and crystal structure on the photocatalytic activity, the photocatalytic degradation tests are carried out (Fig. 6). C_0 and C are the initial concentration after the equilibrium adsorption and the reaction concentration of RhB, respectively. Controll experiment illustrates that the degradation of RhB hardly occurs, while other solutions containing SnO_2 nanocrystals

show photocatalytic degradation in various extents. Comparing the samples **Sn-1/2F**, **Sn-F** and **Sn-2F** with **Sn-0F**, we find that photocatalytic activities are strongly dependent on the dosages of the introduced fluorine ions. The more fluorine ions were introduced, the larger photocatalytic activities of SnO_2 show. The sample **Sn-2F** presents the best photocatalytic activity which shows almost 100% degradation of RhB within 60 min. However, with the dosages of fluorine ions further increased, their photocatalytic activities become much lower than that of **Sn-2F**, even lower than that of **Sn-0F**. In recent years, a few reports have studied the photocatalytic activities of SnO_2 nanostructures in RhB solutions under UV irradiation. By contrast, These SnO_2 nanoparticles we obtained show higher photocatalytic activities when compared with SnO_2 nanostructures perpared by Wu, Wang and their co-workers etc. [10, 22, 40]. The photocatalytic reactions of semiconductor surface are due to the production of photogenerated electrons and holes in the semiconductors by the absorption of UV light. The photocatalytic efficiency depends on the recombination rate or lifetime of photogenerated electrons and holes. If recombination occurs too fast, then there is not enough time for any other chemical reactions to occur [41]. Fluorine ions can serve not only as a mediator of interfacial charge transfer but also as a recombination center [42]. In our study, the fluorine ions on the surface of SnO_2 are believed to be responsible for a reduction of the recombination rate of photogenerated electrons and holes. Fluoride ion has a strong negative, which can make tin atoms positively charged to attract electrons and reduce O_2 into $\cdot O^{2-}$ at the same time. However, a decrease in the photocatalytic activity is observed when excessive fluorine ions are introduced. Maybe the impure crystalline phase existing in the SnO_2 crystals and the narrower absorption bound of UV light are responsible for it.

4. Conclusion

In summary, SnO_2 nanoparticles with small sizes have been synthesized by simple hydrothermal route with existence of different dosages of fluorine ions. Fluorine ions absorbed on SnO_2 nanocrystallines improve the crystallization of rutile phase and promote the growth of crystallites. With R_F increased to 4:1, other impure peaks are found to exist in SnO_2 nanocrystals. A certain amount of fluorine ions are physically adsorbed on the surface of SnO_2 crystals, but not doped in the lattice. The photocatalytic activities of SnO_2 nanoparticles are strongly dependent on the dopant concentration since the fluorine ion can serve not only as a mediator of interfacial charge transfer but also as a recombination center. The sample **Sn-2F** presents the best photocatalytic property. When irradiated under a 300 W high-pressure mercury lamp, the degradation of RhB reaches 100% within 60 min.

References

[1] Elangovan E and Ramamurthi K 2003 J. Optoelectron Adv. M. 1 45-54

[2] Law M, Kind H, Messer B, Kim F and Yang P D 2002 Angew. Chem. Int. Edn. 41 2505-8

[3] Park N, Kang M G, Ryu K S, Kim K M and Chang S H 2003 J. Photochem. Photobiol. A. 161 105-10

[4] Ferrere S, Zaban A and Gregg B A 1997 J. Phys. Chem. B 101 4490-3

[5] Cheng G, Wang J, Liu X and Huang K 2006 J. Phys. Chem. B. 110 16208-11

[6] Cheng G, Chen J Y, Ke H Z, Shang J and Chu R 2011 Mater. Lett. 65 3327-9

[7] Wang G, Lu W, Li J H, Choi J, Jeong Y and Choi S Y 2006 Small 2 1436-9

[8] Han Y T, Wu X, Ma Y L, Gong L H, Qu F Y and Fan H 2011 J. Cryst. Eng. Comm. 13 3506-10

[9] Wang W W, Zhu Y J and Yang L X 2007 Adv. Funct. Mater. 17 59-64

[10] Wu S S, Cao H Q, Yin S F, Liu X W and Zhang X R 2009 J. Phys. Chem. C. 113 17893-8

[11]Jia T K, Wang W M, Long F, Fu Z Y, Wang H and Zhang Q J 2009 J. Phys. Chem. C. 113 9071-7

[12] Chen HH and Xu Y M 2012 J. Phys. Chem. C. 116 24582-9

[13] Zhuang J D, Weng S X, Dai W X, Liu P and Liu Q 2012 J. Phys. Chem. C. 116 25354-61

[14] Nagaveni K, Hegde M S, Ravishankar N, Subbanna G N and Madras G 2004 Langmuir 20 2900-7

[15] Park H and Choi W 2006 Langmuir 22 2906-11

[16] Tseng Y H, KuoC S, Huang C H, Li Y Y, Chou P W, Cheng C L and Wong M S 2006 Nanotechnology 17 2490-7

[17]Sreekantan S, Saharudin K A, Lockman Z and Tzu T W 2010 Nanotechnology 21 365603-10

[18] Slater B, Gay D H, Williams D E and Dusastre V 1999 J. Phys. Chem. B. 103 10644-50

[19] Sinyagin A Y, Belov A, Tang Z and Kotov N A 2006 J. Phys. Chem. B. 110 7500-7

[20] Wen Z H, Wang G, Lu W, Wang Q, Zhang Q and Li J H 2007 Cryst. Growth Des. 7 1722-5

[21] Wang T and Pavle V R 2011 J. Phys. Chem. C. 115 406-13

[22] Kong J T, Shi S Y and Zhu X P 2007 Journal of Environmental Sciences 19 1380-6

[23] Yu K, Zhao Q R and Xie Y 2008 J. Phys. Chem. C. 112 2244-7

[24] Coey J M, Fitzgerald C B and Venkatesan M 2004 Appl. Phys. Lett. 84 1332-4

[25] Zhang K C, Li Y F and Zhu Y 2012 J. Appl. Phys. 112 0437051-5

[26] Elijah T, Martinson B F, Elam J W and Pellin M J 2012 J. Phys. Chem. C. 116 16830–40

[27] Masayoshi Y, Tetsuya K and Kengo S 2012 ACS Appl. Mater. Interfaces. 4 4231-6

[28] Thomas R G, Matteo C, Taejong P, Filippo M, Ralph T W, Paolo F and Christopher B M 2012 J. Am. Chem. Soc. 134 6751-61

[29] Yu J C, Yu J G, Ho W K, Jiang Z T and Zhang L Z 2002 Chem. Mater. 14 3808-16

[30] He Z L, Que W X, Chen J, Yin X T, He Y C and Ren J B 2012 ACS Appl. Mater. Interfaces 4 6816-26

[31] Pan J H, Zhang X W, Du J H, Sun D D and Leckie J O 2008 J. Am. Chem. Soc. 130 11256-7

[32] Zhou J K, Lv L, Yu J Q, Li H L, Guo P Z, Sun H and Zhao X S 2008 J. Phys. Chem. C. 112 5316-21

[33] Wu G S, Wang J P, Thomas D F and Chen A C 2008 Langmuir 24 3503-9

[34] Wang Q, Chen C C, Zhao D, Ma W H and Zhao J C 2008 Langmuir 24 7338-45

[35] Park H and Choi W Y 2004 J. Phys. Chem. B. 108 4086-93

[36] Zhang Z Y, Shao C L, Li X H, Zhang L, Xue H M, Wang C H and Liu Y C 2010 J. Phys. Chem. C. 114 7920-5

[37] Peng X S, Meng G W, Wang X F, Wang Y W, Zhang J, Liu X and Zhang L D 2002 Chem. Mater. 14 4490-3

[38] Cheng G, Wu K, Zhao P T, Cheng Y, He X L and Huang K X 2007 Nanotechnology 18 355604-10

[39] Yu J C, Yu J, Ho W, Jiang Z and Zhang L 2002 Chem. Mater. 14 3808-16

[40] Han Y T, Wu X, Ma Y L, Gong L H, Qu F Y and Fan H J 2011 Cryst. Eng. Comm. 13 3506–10

[41] Yu J G, Wang W G, Cheng B and Su B L 2009 J. Phys. Chem. C. 113 6743-50

[42] Yu J G, Xiang Q J, Ran J G and Mann S 2010 Cryst. Eng. Comm 12 872-9

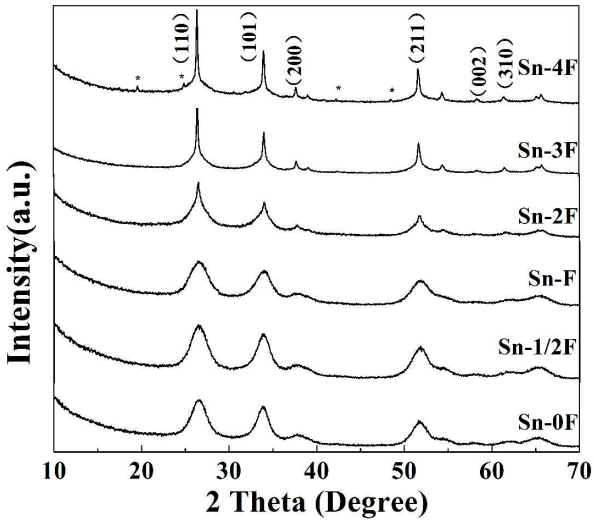

Fig. 1. The XRD pattern of the as-obtained products

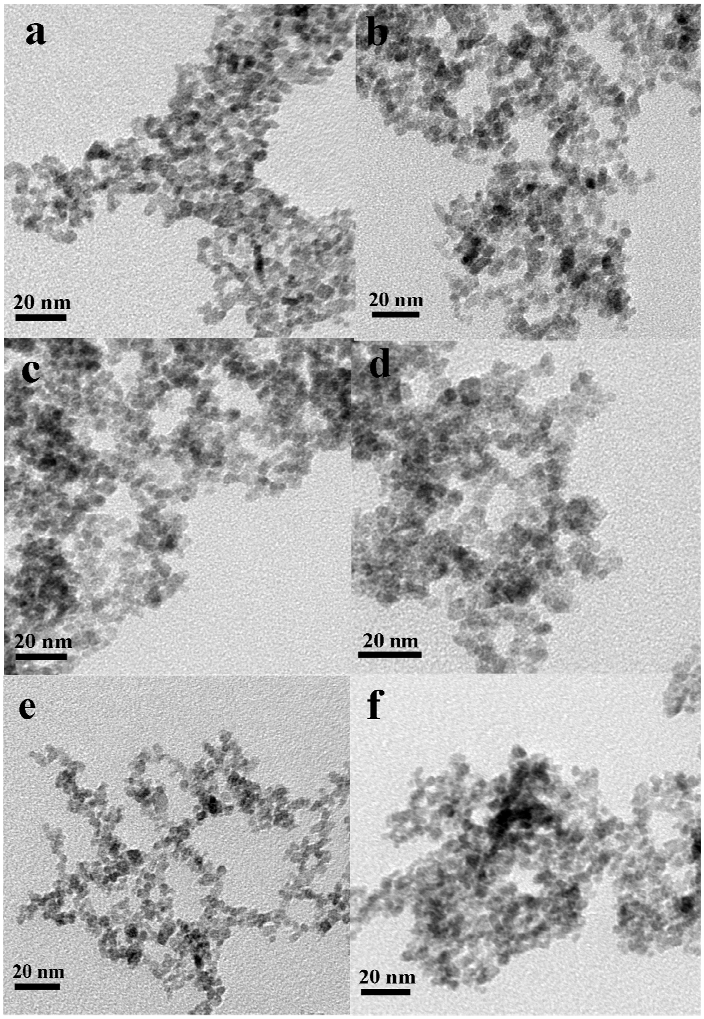

Fig. 2. TEM images of the as-obtained products: (a) **Sn-0F**; (b) **Sn-1/2F**; (c) **Sn-F**; (d) **Sn-2F**; (e) **Sn-3F**; (f) **Sn-4F**

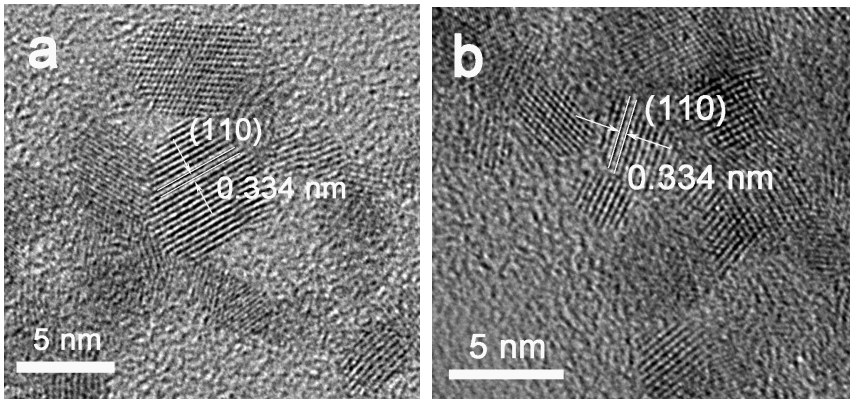

Fig. 3. The HRTEM images of SnO_2 nanoparticles: (a) **Sn-0F**; (b) **Sn-2F**

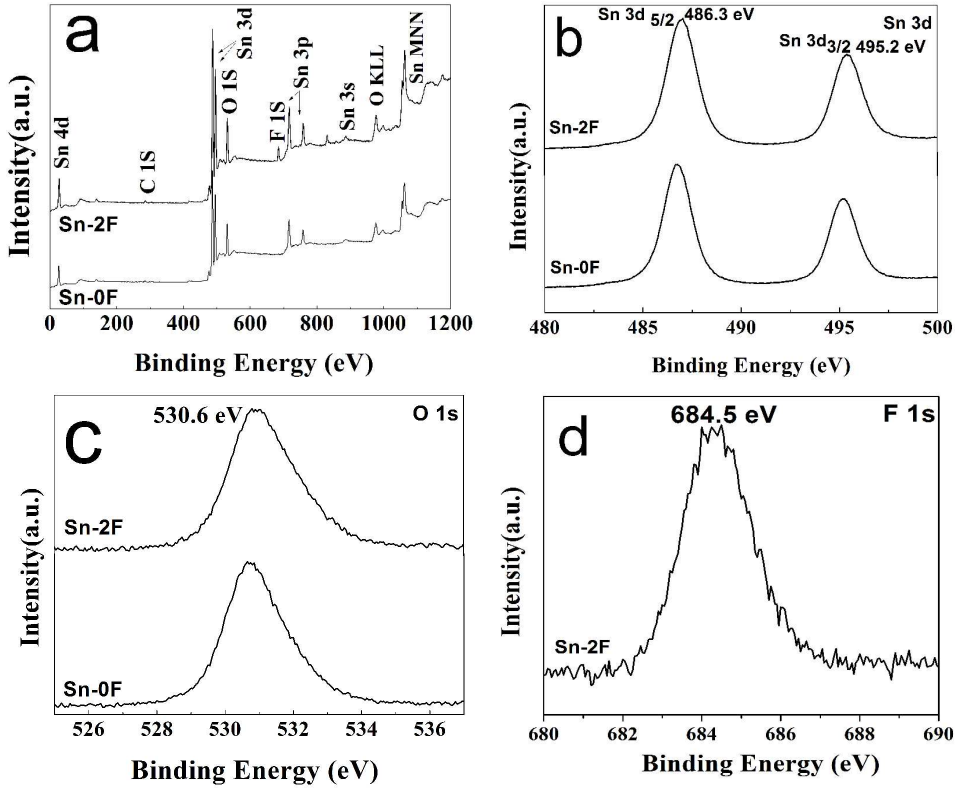

Fig. 4. The high-resolution XPS spectra of **Sn-0F** and **Sn-2F:** (a) XPS full spectrum; (b) Sn 3d; (c) O 1s ;(d) F 1s

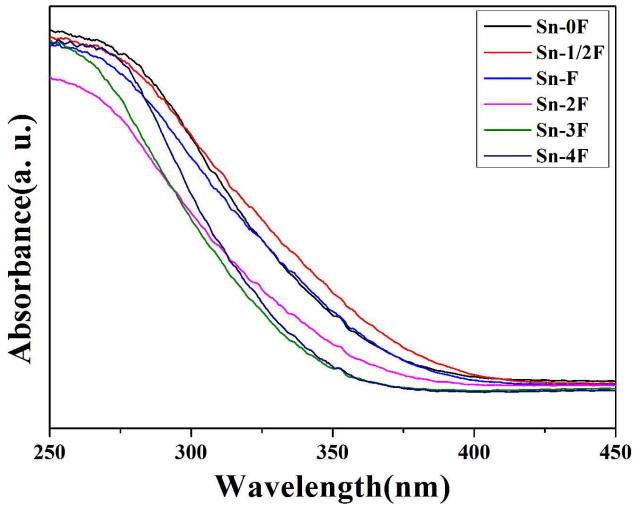

Fig. 5. The UV-Visible diffuse reflectance spectra (DRS) of all samples

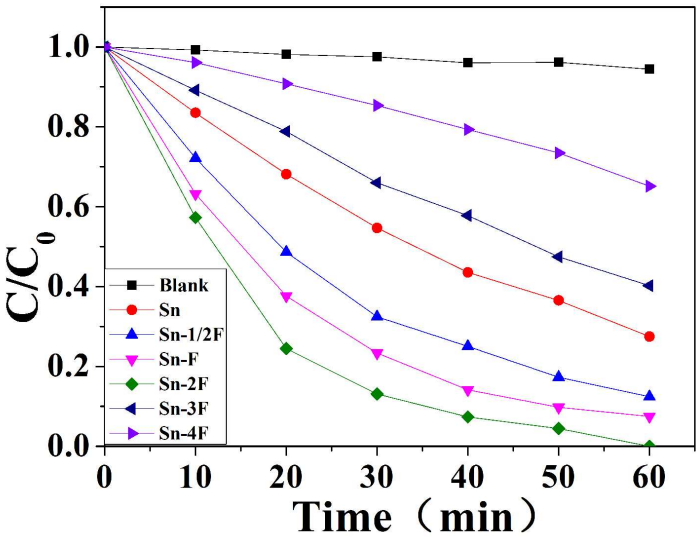

Fig. 6. Degradation curves of RhB under UV irradiation in the presence of various photocatalysts